Evaluation of Models for Tubular, Laminar Flow Reactors

THEODORE S. ANDERSEN and JAMES COULL

University of Pittsburgh, Pittsburgh, Pennsylvania

Significant error can result when the plug flow model is applied to the analysis or design of laminar flow reactors due to nonconstant radial profiles of velocity, composition, and temperature.

An analysis and comparison of suitable models for the nonisothermal, homogeneous, first-order, irreversible, laminar, gas flow reactor has shown the finite-difference solution for radial profiles to be superior to the power-series approximation of radial temperature and composition profiles.

New capabilities of the present computer solution include isothermal or adiabatic wall, dilute or concentrated feed, any stoichiometric product-to-reactant ratio, Chapman-Enskog model for gas diffusivity, calculation of both heat transfer parameters, and a correction factor to apply to plug flow calculations.

The new, improved computer solution may be used in the basic design or analysis of tubular, laminar flow reactors.

Until recently, usual chemical engineering practice assumed plug flow conditions for the design and analysis of all homogeneous flow reactors. The details of this type of analysis are given by Hougen and Watson (*1*). Although the plug flow assumption is quite good when the reactant is flowing in the turbulent regime, significant error can be introduced when it is applied to systems in the laminar regime.

Sandler and Chung (*2*) provide experimental evidence of the error in their study of the kinetics of the pyrolysis of butane in a laminar flow reactor. The overall reaction rate which they determined by assuming plug flow conditions is significantly different than that reported by Steacie and Puddington (*3*) which was based on a small bulb batch type of reactor.

The laminar flow regime differs from plug flow in several important ways. Radial temperature gradients exist and cause a variation in reaction rate over the cross section of the reactor. Radial concentration gradients exist and cause radial molecular diffusion which noticeably influences heat transfer to the reactor. Radial gradients of the axial velocity exist which cause each cylindrical shell of reacting fluid to have a different residence time in the reactor.

Cleland and Wilhelm (*4*) represented an isothermal laminar flow reactor analytically and solved for the concentration profiles numerically. The results of their work described the effects of the radial gradients of concentration and axial velocity.

Two separate and basically different analyses have been published recently which account for radial gradients in temperature, concentration, and axial velocity.

1. Trombetta and Happel (*5*) studied the analysis and design of gas flow reactors with applications to hydrocarbon pyrolysis. They presented their results as factors which can be used to correct calculations made with the plug flow assumption.

2. Rothenberg and Smith (*6*) studied heat transfer and reaction in laminar tube flow. They gave particular attention to the effect reaction and diffusion had on the heat transfer characteristics of the reactor.

Theodore S. Andersen is with Westinghouse Electric Corporation, Bettis Atomic Power Laboratory, West Mifflin, Pennsylvania.

The prime objective of this work (*7*) is the comparison of the two different solutions of references 5 and 6 to the analysis of a tubular, laminar flow, homogeneous, first-order, irreversible, gas-phase reactor. This comparison cannot be made trivially because of the very different ways used by the separate authors to represent the results.

The method of comparison chosen is straightforward. Basic equations used by Rothenberg and Smith were generalized, and a similar digital computer solution was sought. Results of the calculations were then used to calculate all of the quantities reported in both references 5 and 6. Limitations and underlying assumptions of both previous analyses and the present one are summarized in Table 1.

MATHEMATICAL MODEL

Once the basic equations of the system are derived from the general equations of continuity, motion, and energy, two approaches to the solution are possible. The present work follows a solution of the type presented by Rothenberg and Smith. A short analysis of the alternate solution of Trombetta and Happel is also presented to define the basic differences in approach. Several useful quantities are derived from the solution which is in the form of radial temperature and reactant concentration profiles.

Basic Equation

The basic equations are derived from the complete transport equations as given by Bird, Stewart, and Lightfoot (*8*) by elimination of terms in accordance with the physical aspects of the system. These equations are based on only those assumptions common to both approaches.

Continuity of the total mass of the axissymmetric, steady state system may be expressed in cylindrical coordinates as

$$\frac{\partial}{r\partial r}(r\rho v_r) + \frac{\partial \rho v_z}{\partial z} = 0 \qquad (1)$$

Continuity for the number of moles of species i can similarly be expressed:

$$\frac{\partial}{r\partial r}(r N_{ir}) + \frac{\partial N_{iz}}{\partial z} = R_i \qquad (2)$$

The molar flux is the sum of the convective and molecular

diffusion fluxes in the absence of appreciable thermodynamically cross-coupled terms:

$$N_i = C_i\, v^* + J_i \tag{3}$$

Now, if the axial molecular diffusion can be assumed to be much less than the axial convective flow, $N_{iz} = C_i\, v_z^*$ and Equation (2) can be written as

$$\frac{\partial}{r\partial r}\left(r\, C_i\, v_r^* + r\, J_{ir}\right) + \frac{\partial}{\partial z}\left(C_i\, v_z^*\right) = R_i \tag{4}$$

The equation of motion may be written in the boundary-layer form used by Trombetta if J_{ir} is radially uniform, if the axial gradient of v^* is much smaller than the radial gradient, and if v_z is much greater than v_r, as may be expected for flow in a parallel walled conduit:

$$\frac{\partial p}{\partial r} = 0 \tag{5}$$

$$v_r \frac{\partial \rho v_z}{\partial r} + v_z \frac{\partial \rho v_z}{\partial z} = \frac{-\partial p}{\partial z} - \mu \frac{\partial}{r\partial r}\left(\frac{r\partial v_z}{\partial r}\right) \tag{6}$$

The equation of energy for the system is also subject to several conditions: the change in energy by kinetic, dissipative and radiant effects is negligible, thermodynamic coupling (Dufour effect) is not significant, and both the thermal conductivity and mass specific heat are constant throughout the system:

$$\sum_i \mathrm{H}_i R_i = k\left(\frac{\partial^2 T}{\partial r^2} + \frac{\partial T}{r\partial r}\right) - \sum_i \tilde{c}_{pi}\left(N_{ir}\frac{\partial T}{\partial r} + c_i\, v_z^* \frac{\partial T}{\partial z}\right) \tag{7}$$

The reaction is assumed to be irreversible and first order with respect to the single reactant, represented by

$$A \rightarrow bB \tag{8}$$

where $b = \Sigma b_i$ is the total number of moles of product per mole of reactant, and

$$B = \frac{1}{b}\sum_i b_i\, B_i$$

if there are two or more products. The rate of generation of the products is then

$$R_B = -b\, R_A = b\, K\, c_A \tag{9}$$

The Arrhenius relation is assumed for K:

$$K = F\, \exp\left(-E/R_g T\right) \tag{10}$$

The enthalpy change of the reaction may be expressed as

$$\Delta \mathrm{H}^0 = \mathrm{H}_A - b\mathrm{H}_B \tag{11}$$

where H_B is defined similarly to B for Equation (8).

The initial temperature and composition profiles at $z = 0$ are taken as being uniformly constant:

$$T = T_0, \quad y = y_0 \quad \text{at} \quad z = 0 \tag{12}$$

The boundary conditions at the center line of the reactor result from cylindrical symmetry:

$$N_{ir} = \frac{\partial T}{\partial r} = 0 = \frac{\partial y}{\partial r} = 0 \text{ for all } i \text{ at } r = 0 \tag{13}$$

Also, at the center line by L'Hospital's rule

$$\frac{\partial T}{r\partial r} = \frac{\partial^2 T}{\partial r^2}, \quad \frac{\partial y}{r\partial r} = \frac{\partial^2 y}{\partial r^2} \quad \text{at} \quad r = 0 \tag{14}$$

Several conditions may occur at the reactor wall, $r = R$. If the wall temperature is held constant at T_0

$$T = T_0 \quad \text{at} \quad r = R \tag{15}$$

However, if the reactor is operated adiabatically, the radial heat flux at the wall is zero:

$$\frac{\partial T}{\partial r} = q_r = 0 \quad \text{at} \quad r = R \tag{16}$$

If the wall is inert and impermeable, the radial molar flux is zero:

$$\frac{\partial y_i}{\partial r} = N_{ir} = 0 \quad \text{for all } i \quad \text{at } r = R \tag{17}$$

Other wall constraints such as specified variations in fluxes or temperature or concentrations are equally amenable to the solution but have not been analyzed in this study.

Approach to Solution

Three basic assertions are made which enable the simplification of the basic equations to a point where a straightforward numerical solution of the problem is possible. Dimensionless quantities are introduced to further simplify the expressions obtained. Several useful quantities are derived from the basic properties of temperature and reactant concentration.

Definitions of useful dimensionless variables are given below; the particular convenience of each will become clear in the development of the final equations:

Radial position	r^+	=	r/R_0
Axial position	z^+	=	$z/R_0 N_{Re} N_{Pr}$
Reactant mole fraction	y^+	=	y/y_0
Average molecular weight	M^+	=	M/M_0
Temperature	T^+	=	$(T - T_0)/T_0$
Lewis number	G_1	=	$c_p M_0 c D^0{}_{AB}/k$
Activation energy group	G_2	=	$E/R_g T_0$
Frequency factor group	G_3	=	$R_0{}^2 M_0 c_p P_T F/k$
Heat of reaction group	G_4	=	$-\Delta \mathrm{H} y_0/M_0 c_p T_0$
Damkohler number	N_{Da}	=	$G_3 \exp(-G_2)$
Reynolds number	N_{Re}	=	$2R_0 w/\mu$
Prandtl number	N_{Pr}	=	$c_p \mu/k$

(18)

The effective binary diffusion coefficient for the reactant in the product may be expressed as the stoichiometrically weighted average of the several binary diffusion coefficients:

$$D_{AB} = (\Sigma\, b_i\, D_{ABi})/b \tag{19}$$

Trombetta and Happel concluded this to be an adequate approximation in place of solving the multicomponent diffusion equations.

The commonly assumed conditions of parabolic velocity profile and stoichiometric counter diffusion have been justified empirically by Trombetta and Happel. These two assumptions will be used here, and their close relation to each other will be demonstrated. The radial mass averaged velocity is given by

$$v_r = (M_A\, N_{Ar} + M_B\, N_{Br} + M_I\, N_{Ir})/\rho \tag{20}$$

and the statement of the parabolic velocity profile is

$$v_z = \frac{2w}{\rho}\left[1 - (r^+)^2\right] \tag{21}$$

Substitution of (21) into the equation of continuity (1) requires $v_r = 0$.

TABLE 1. COMPARISON OF MODELS

Basic assumptions and options	Rothenberg and Smith	Trombetta and Happel	Present
Flow regime: steady state, laminar	Yes	Yes	Yes
Single phase	Gas or liquid	Gas	Gas
Reaction: first-order, irreversible	Exothermic and endothermic	Endothermic only	Exothermic and endothermic
Distinct reaction products	1	2	1
Significant change in total number of moles	No	Yes	Yes
Presence of inert diluent	Yes	No	Yes
Diffusion equations	Equivalent binary	Ternary	Equivalent binary
Stoichiometric diffusion	Yes	No	Yes
Arrhenius temperature dependence of reaction rate constant	Yes	Yes	Yes
Temperature dependence of diffusivity	None	None	Chapman-Enskog gas model
Temperature dependence of total molar density	None	Ideal gas	Ideal gas
Radial temperature and concentration profiles	Determined numerically	Analytically fit to series	Determined numerically
Reaction rate determined numerically	Point by point	Radially averaged	Point by point
Wall boundary conditions	Isothermal	Isothermal	Isothermal or adiabatic
Reactor geometry	Tubular	Tubular or annular	Tubular
Calculational accuracy	Variable by increment size	Fixed by selection of power series	Variable by increment size
Nusselt numbers given	Yes	No	Yes
Correction factors given	No	Yes	Yes

The assertion of stoichiometric diffusion may now be made if the assumption that inert diluents do not diffuse radially ($N_{Ir} = 0$) is allowed. Equation (20) would then become

$$M_A N_{Ar} + M_B N_{Br} = 0$$

or

$$N_{Br} = -\frac{M_A}{M_B} N_{Ar} = -b N_{Ar} \tag{22}$$

which is the statement of stoichiometric diffusion.

Final Equations

With the simplifying assertions described, the basic equations of the system may be reduced to two simultaneous differential equations in temperature and reactant concentration.

The equation of continuity (4) may be rewritten by considering effective binary diffusion:

$$N_{Ar} = y\,(N_{Ar} + N_{Br}) - cD_{AB}\frac{\partial y}{\partial r} = -cD_{AB}\frac{\partial y}{\partial r}/[1 + y\,(b-1)] \tag{23}$$

$$N_{Az} = c_A v_z^* = y\frac{v_z}{M} \tag{24}$$

Then, Equation (4) becomes

$$\frac{-\partial}{r\partial r}\left[\frac{rc\,D_{AB}\frac{\partial y}{\partial r}}{1 + y\,(b-1)}\right] + \frac{\partial}{\partial z}\left(\frac{y\rho v_z}{M}\right) = R_A \tag{25}$$

Bird, Stewart, and Lightfoot give the variation of cD_{AB} with temperature according to the Chapman-Enskog kinetic theory of gases as $cD_{AB} = (cD_{AB})^0 T^{3/2}$. The average molecular weight of the reacting solution may be expressed as a function of the extent of reaction when a large fraction of the total number of moles in a streamline are present by (axial) convection:

$$M^+ = \frac{1}{[1 + \xi\,(b-1)y_o]} = \frac{1 + y_o y^+ (b-1)}{1 + y_o(b-1)} \tag{26}$$

With these relations and the equations of motion (21) and reaction (10), continuity (25) becomes in dimensionless variables

$$\left\{\frac{G_1(T^+ + 1)^{0.5}}{1 + y_o y^+ (b-1)}\left[\frac{\partial^2 y^+}{\partial r^{+2}} + \left(\frac{1}{r^+} + \frac{1}{2(T^+ + 1)}\frac{\partial T^+}{\partial r^+} - \frac{y_o(b-1)}{1 + y_o y^+ (b-1)}\frac{\partial y^+}{\partial r^+}\right)\left(\frac{\partial y^+}{\partial r^+}\right)\right] - G_3 y^+ \exp\left(\frac{-G_2}{T^+ + 1}\right)\right\}\frac{[1 + y_o y^+ (b-1)]^2}{1 - y_o(b-1)} = (1 - r^{+2})\frac{\partial y^+}{\partial z^+} \tag{27}$$

Similarly, the equation of energy (7) may be rewritten in dimensionless terms after combination with the equations of motion, reaction, and stoichiometric diffusion:

$$(1 - r^{+2})\frac{\partial T^+}{\partial z^+} = \frac{\partial^2 T^+}{\partial r^{+2}} + \frac{\partial T^+}{r^+\,\partial r^+} + G_3 G_4 y^+ \exp\left(\frac{-G_2}{T^+ + 1}\right) \tag{28}$$

Derived Quantities

The comparison made between the present work and that of Rothenberg and Smith is based mainly on the bulk temperature and reactant concentration curves which they published. The comparison is made with the work of Trombetta and Happel through their correction factor curves. Expressions are now derived for these quantities, as well as wall heat flux and Nusselt number, from the radial distributions which can be obtained by solving Equations (27) and (28).

The bulk properties were defined by Rothenberg and Smith as the properties which result when the fluid at a particular axial position is mixed at constant enthalpy and no further reaction occurs. Physically, the bulk property is the mass velocity weighted property averaged over the flow area:

$$T_b^+ = \frac{2\int_0^1 v_z T^+ r^+ dr^+}{2\int_0^1 v_z r^+ dr^+} = \frac{\int_0^1 2G(1-r^{+2})T^+ r^+ dr^+}{\int_0^1 2G(1-r^{+2})r^+ dr^+} \tag{29}$$

$$T_b^+ = 4\int_0^1 (r^+ - r^{+3})T^+ dr^+ \tag{30}$$

Similarly, for the bulk reactant concentration

$$y_b^+ = 4\int_0^1 (r^+ - r^{+3})y^+ dr^+ \tag{31}$$

The integrals in Equations (30) and (31) can be evaluated numerically.

Two techniques are available to calculate the wall heat flux. Both calculations were made and favorably compared.

1. A differential shell balance may be established near the wall if axial transport of energy is negligible at the wall. The energy balance may then be written as a balance of radial fluxes

$$q_{R_o} = -k\left(\frac{\partial T}{\partial r}\bigg|_{R_o} + \frac{\text{H}\, D_{AB}}{1+(b-1)y}\left(\frac{\partial y}{\partial r}\bigg|_{R_o}\right.\right. \tag{32}$$

or, equivalently, by rearranging and with dimensionless variables:

$$q^+ = \frac{2R_o q_R}{kT_0} = -2\left[\left(\frac{\partial T^+}{\partial r^+}\bigg|_{R_o} - \frac{2G_1G_4}{1+(b-1)y_0y^+}\right)\left(\frac{\partial y^+}{\partial r^+}\bigg|_{R_o}\right)\right] \tag{33}$$

2. A differential disk balance may be established over the entire flow area. For this case, Equation (26) becomes exact when the bulk values of concentration are used, because there is no net radial flow in the total system. The disk energy balance may then be written as

$$q_b = \frac{-R_o^2 G}{2R_o}\left(c_p\frac{dT_b}{dz} - \Delta\frac{\text{H}d(y_b/M)}{dz}\right) \tag{34}$$

or, equivalently, by rearranging and with dimensionless variables:

$$q_b^+ = \frac{2R_o q_b}{kT_0} = \frac{dT^+}{2dz^+} - \frac{G_4[1+y_0(b-1)]}{2[1+y_0y^+(b-1)]^2}\frac{dy^+}{dz^+} \tag{35}$$

The Nusselt number is defined as

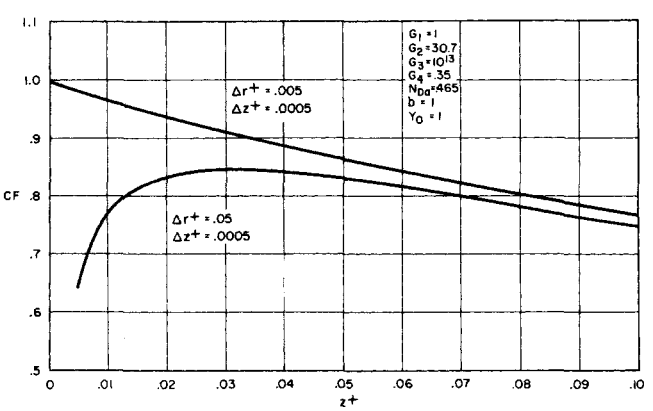

Fig. 1. The effect of increment size on the correction factor calculation.

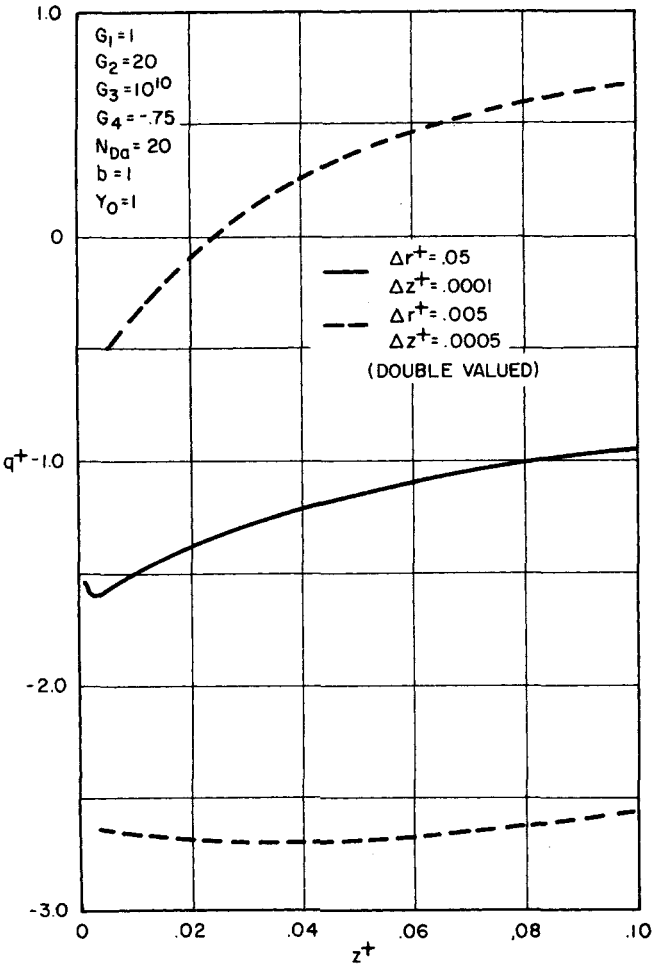

Fig. 2. The effect of increment size on the heat flux calculation.

$$N_{Nu} = \frac{2qR_o}{k\Delta T} \tag{36}$$

Rothenberg and Smith described both a point Nusselt number, based on the heat flux and temperature difference at a specific axial position, and an average Nusselt number, based on the heat flux integrated along the length of the reactor and the arithmetic mean temperature difference.

1. The point Nusselt number may be evaluated simply from the parameters previously described:

$$N_{Nup} = \frac{q^+}{T_b^+ - T_R^+} \tag{37}$$

2. The average Nusselt number, by its definition, is

$$N_{Nua} = \frac{2\int_0^{z^+} q_b^+ dz^+}{z^+(T_0^+ - T_0^+ + T_b^+ - T_{R_o}^+)} \tag{38}$$

which becomes upon integration

$$N_{Nua} = \frac{-T_b^+ + G_4\left(\dfrac{1-y_b^+}{1+y_0y_b^+(b-1)}\right)}{z^+(T_b^+ - T_{R_o}^+)} \tag{39}$$

The equivalent plug flow reactor length z'' is defined by Trombetta and Happel as being the length of an isothermal plug flow reactor which will produce the same bulk reactant concentration as the reactor being considered. It may be found by setting all derivatives with respect to r^+ and T^+ equal to zero in the continuity equation for the reacting species (27):

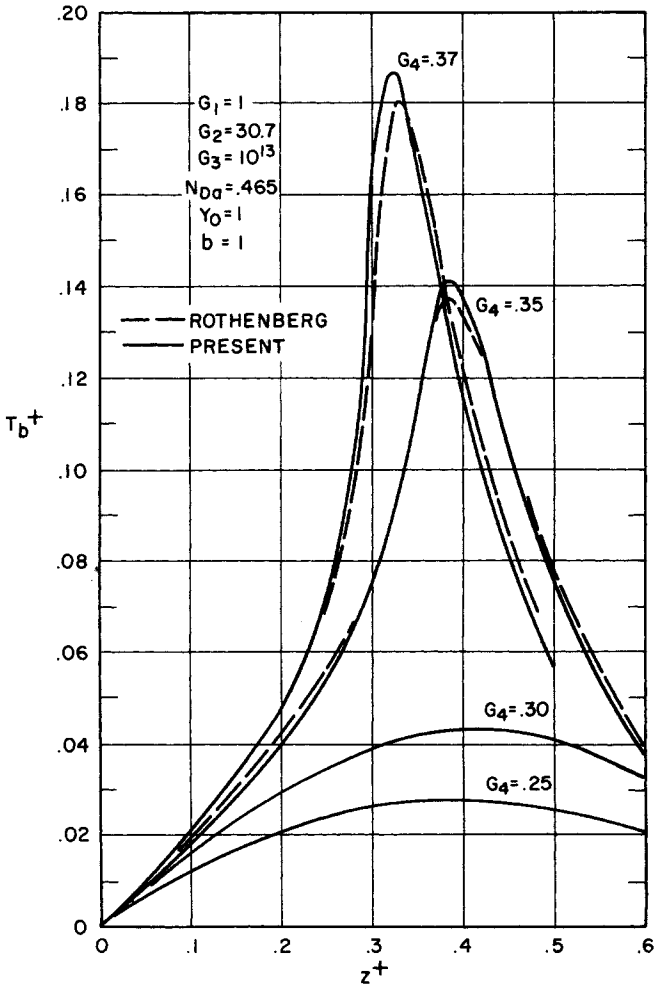

Fig. 3. Axial temperature profiles for exothermic reactions.

$$(1 - r^{+2}) \frac{dy^+/M}{dz^+} = - G_3 y^+ \exp(-G_2) = N_{Da} y^+ \tag{40}$$

Finding the bulk value of $\left(d \frac{y^+}{M^+} / dz^+ \right)$ and then integrating along the axis, we obtain

$$\int_1^{y_b^+} \frac{1 + y_0(b-1)}{y_b^+[1 + y_0 y_b^+ (b-1)]^2} dy_b^+ = -2 \int_0^{z''} N_{Da} dz^+ \tag{41}$$

$$z'' = \frac{-1}{2N_{Da}} \left[\frac{y_0(b-1)(1-y_b^+)}{1 + y_0 y_b^+ (b-1)} + [1 + y_0(b-1)] \ln \left[\frac{y_b^+(1 + y_0(b-1))}{1 + y_0 y_b^+ (b-1)} \right] \right] \tag{42}$$

Trombetta and Happel defined the correction factor simply as the ratio of the true reactor length to the equivalent plug flow reactor length:

$$CF = z^+/z'' \tag{43}$$

An Alternate Solution

Trombetta and Happel presented a different solution to the same basic equations. Details may be found in reference 5, but a brief outline will be given here to demonstrate the basic differences.

The same basic equations were used: continuity (4), motion (5) and (6), energy (7), and reaction (10). Two products were assumed for the reaction, and ternary diffusion equations were used to describe the diffusive mass fluxes. Disk balances were then written for continuity, momentum, and energy.

Solutions for concentrations and temperature were assumed:

$$y^+ = Z_7(z) + Z_8(z)(r^{+2} - r^{+4}) + Z_9(z)\left(r^{+6} - \frac{3r^{+4}}{2}\right) \tag{44}$$

$$T^+ = Z_1(z)(1 - r^{+2}) + Z_2(z)(r^{+4} - r^{+2}) = Z_3(z)(r^{+6} - r^{+2}) \tag{45}$$

where the Z's are functions of axial position only. These polynomials were then substituted into the integral and differential equations described above. Twelve simultaneous ordinary differential equations in the twelve unknowns (Z_1-Z_{12}) were thus derived.

The Gaussian elimination technique was used to solve the set of equations at each axial position (average reaction rate had to be evaluated by numerical integration). The Runge-Kutta method was then applied to integrate axially. Trombetta and Happel presented the results of their analysis in terms of the correction factor defined in Equation (43).

In the discussion of results, Trombetta and Happel concluded that:

1. Diffusion in a two-product reaction system may be

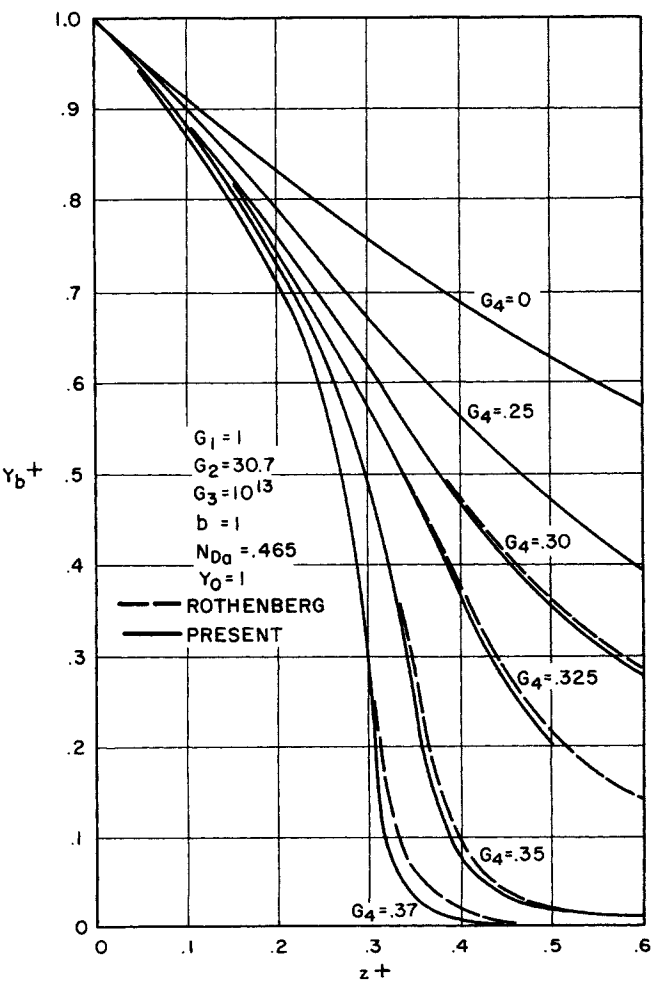

Fig. 4. Axial reactant concentration profiles for exothermic reactions.

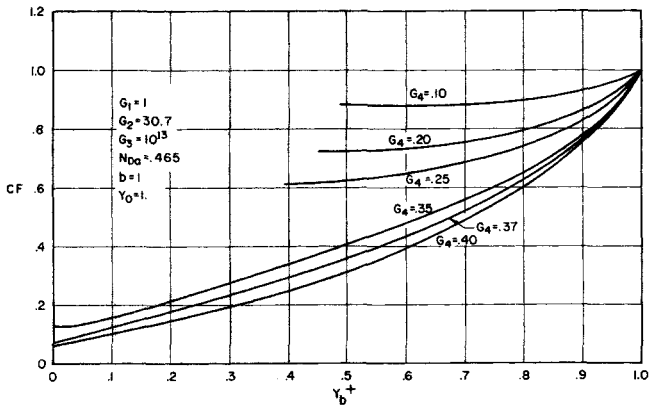

Fig. 5. Correction factors for exothermic reactions.

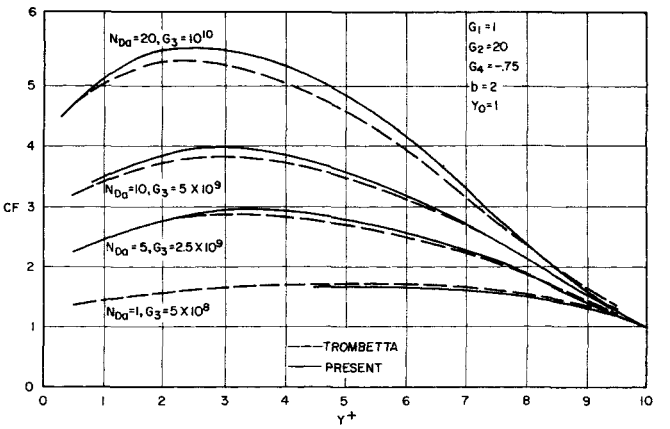

Fig. 6. Correction factors for endothermic reactions.

adequately represented by the effective binary diffusion coefficient defined in Equation (19).

2. The velocity profile may be identically assumed parabolic.

NUMERICAL SOLUTION

The solution of the simultaneous partial-differential equations derived above were found by applying the implicit Crank-Nicolson technique used by Rothenberg and Smith. This same approach to the solution is given by Lapidus (9) for the isothermal case (the same problem solved by Cleland and Wilhelm).

Basically the technique consists of expressing all derivatives in terms of finite-difference approximations, of establishing a tridiagonal matrix of a physical variable at the next axial increment, and of solving for the physical variable at each mesh point in terms of its values at the previous axial position. Details of the solution are presented in reference 7.

Properties of the Numerical Solution

The numerical solution used becomes exact only as the radial and axial increments become infinitesimal. Unfortunately, modern digital computer hardware imposes the limitation of finite increments; a compromise must be found between precision, core storage capability, and problem running time.

Rothenberg and Smith typically used ten radial increments and an axial increment size between 0.00025 and 0.01, with a running time of approximately 25 min. for 125 axial increments. They observed that a minimum ratio of $\Delta z^+/\Delta r^+$ is necessary for a stable solution.

Improved computer technology has made much smaller increments practical; the present investigation (conducted on an IBM-7090) included problems with 200 radial increments, $\Delta z^+ = 0.0001$ with 1,000 axial increments processed in 15 min. Less demanding problems ran in correspondingly less time with twenty radial increments and 1,000 axial increments typically running 2 min.

Two calculated parameters were found to be particularly sensitive to the increment sizes in the present investigation near the reactor entrance.

The correction factor is very sensitive to Δr^+. This sensitivity arises because small errors in the numerical radial integration to obtain $Y_b{}^+$ are greatly magnified by the calculation of CF at small axial distances from the entrance. Twenty radial increments proved inadequate to define CF at small z^+; 200 radial increments proved quite satisfactory as shown in Figure 1.

The radial heat flux is sensitive to the ratio $\Delta z^+/\Delta r^+$. For a too large value of the ratio, the calculated value of q^+ oscillates markedly from point to point. Although the critical value of the ratio depends on the rate and heat of reaction, a generally acceptable value was found to be 0.02 (see Figure 2).

These two requirements for a precise solution combine to require a very small Δr^+ and a proportionately smaller Δz^+. With the practical limitation of 1,000 axial increments, reactions cannot be followed with high precision over a comprehensive range of reactant concentrations. An adequate solution was found by using the high precision where most needed, near the reactor entrance.

Results of a short, fine-mesh analysis ($\Delta r^+ = 0.005$, $\Delta z^+ = 0.0001$) at the reactor entrance (to $z^+ = 0.02$) were used as the initial conditions to a longer, medium-mesh solution ($\Delta r^+ = 0.01$, $\Delta z^+ = 0.0002$); these results were then used as the initial conditions for a third, coarse-mesh solution to exhaust the reactant ($\Delta r^+ = 0.10$, $\Delta z^+ = 0.005$). The values given above were for a particular problem, but they are typical; running time for the continuation type of problems was typically 8 min. for 600 total axial increments. Results at the end of the medium-mesh solution (400 total axial increments) were not found to be significantly different from those calculated for an equivalent reaction by using only fine-mesh for 1,000 axial increments.

EVALUATION OF THE MODEL

Results obtained from the present model demonstrate excellent agreement with the model of Rothenberg and

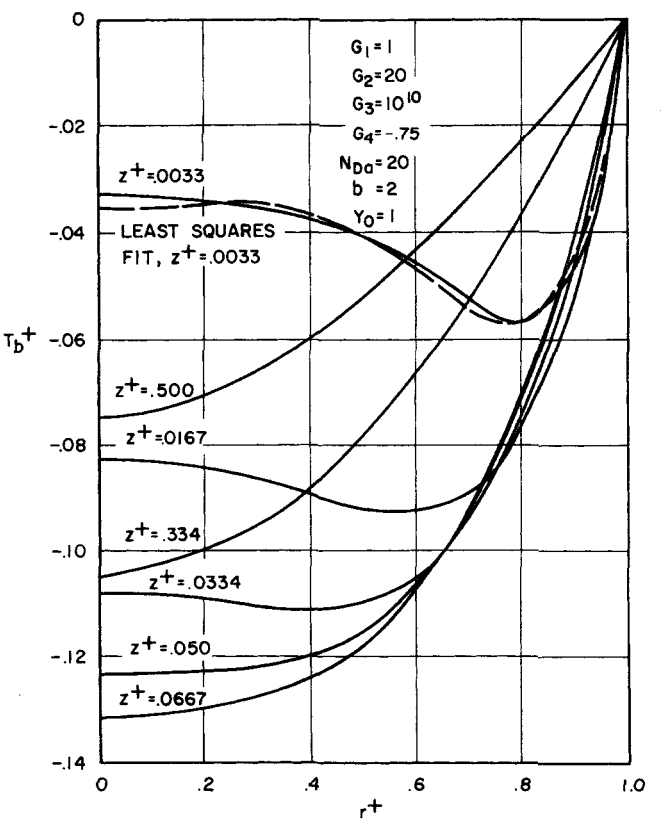

Fig. 7. Radial temperature profiles for an endothermic reaction.

Smith and good agreement with that of Trombetta and Happel. Several of the unique features of the present model were found to be significant improvements over the previous models. The experimental results of Sandler and Chung were predicted successfully within the experimental uncertainty.

Comparison with the Rothenberg and Smith Model

Figures 3 and 4 illustrate the comparison of axial temperature and reactant concentration profiles; where a visible difference exists, the broken curve is that of Rothenberg and Smith. The probable reason for the slightly higher temperature peaks and lower concentrations of the present analysis is finer resolution due to a finer calculational mesh. Unfortunately, Rothenberg and Smith did not publish mesh dimensions for particular analyses which could be used for a specific comparison.

The axial Nusselt number profiles derived for these conditions were essentially identical to those presented by Rothenberg and Smith. Radial temperature and concentration profiles calculated by the present method also agreed well with those presented in reference 6.

The correction factors presently calculated for the conditions assumed by Rothenberg and Smith are shown in Figure 5. As would be expected, the necessary length of a laminar flow reactor with exothermic reaction can be considerably less than that calculated by the initial temperature, isothermal, plug flow assumption. The correction factors approach a limit of unity both at the reactor entrance, where the isothermal assumption is exact, and at the point of total reactant exhaustion, where all heat of reaction is dissipated and again the isothermal assumption approaches reality.

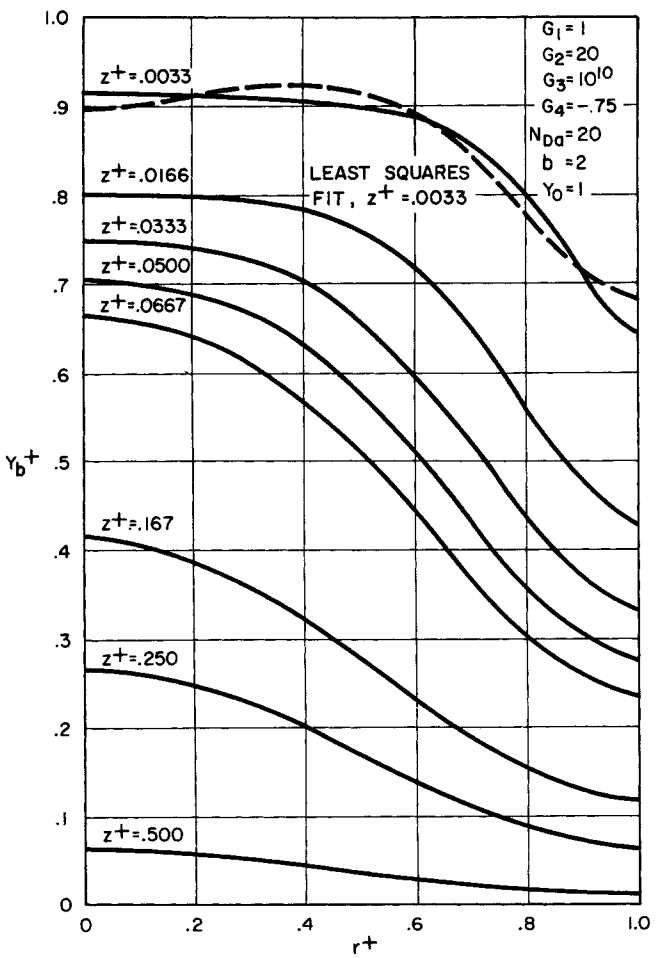

Fig. 8. Radial reactant concentration profile for an endothermic reaction.

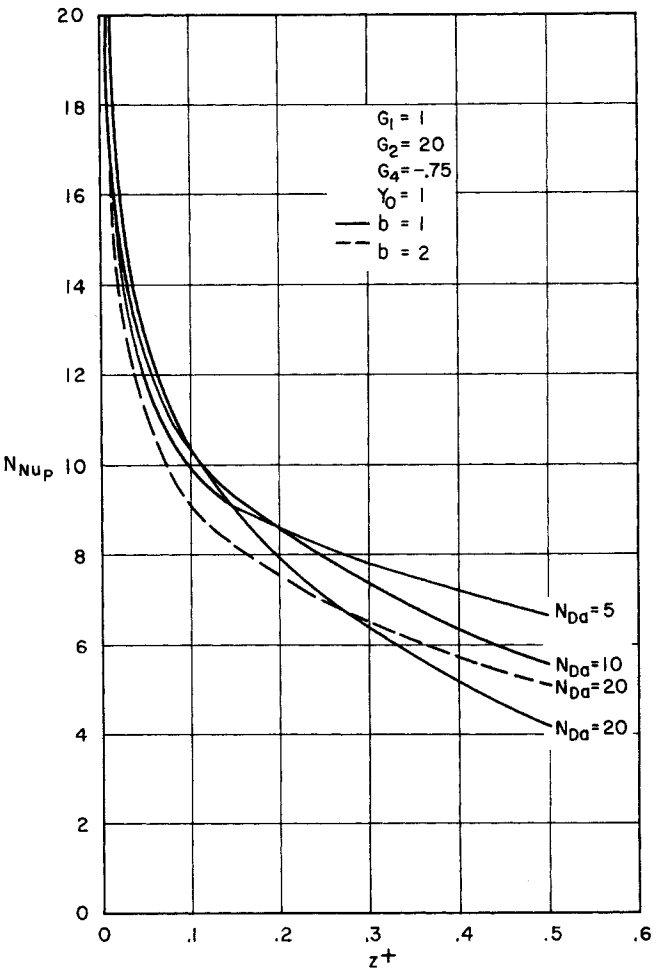

Fig. 9. Point Nusselt numbers for endothermic reactions.

No attempt has been made to duplicate all the work reported by Rothenberg and Smith. They also investigated the effects of variations of the dimensionless parameters and suggested a method to analyze liquid systems.

Comparison with Trombetta and Happel Model

Figure 6 illustrates the comparison of correction factors published by Trombetta and Happel with the present work. Similar comparisons are made in reference 7 for other curves of reference 6. At the higher values of Damkohler number, the present values are up to 5% higher and at low Damkohler number up to 5% lower than the values of Trombetta and Happel. This is within the estimated calculational uncertainty of 6% reported by Trombetta and Happel for their method. In an attempt to discover whether the discrepancy arose because of the form of radial profiles assumed by Trombetta and Happel, equations of the form of Equations (44) and (45) were fitted to 200 points, presently calculated for several radial profiles, by the least-squares method.

The radial temperature and concentration profiles derived (for $z^+ = 0.0033$) are presented in Figures 7 and 8. The power series cannot fit the derived temperature profile exactly and thus is somewhat more restrictive than the present analysis.

Trombetta and Happel compared their solution for the case of zero heat of reaction with correction factors calculated from the results of Cleland and Wilhelm, which they considered exact. The present work is added to the

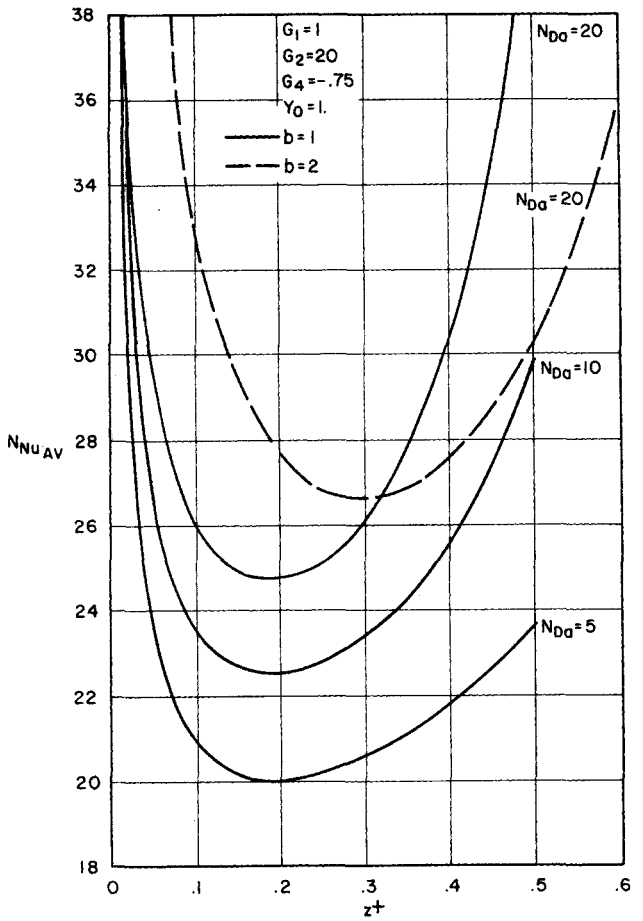

Fig. 10. Average Nusselt numbers for endothermic reactions.

comparison in Table 2. Actually, Cleland and Wilhelm found an analytic solution only for the case of zero diffusion or infinite reaction rate ($N_{Da}/G_1 = \infty$), but their numerical solution for other conditions approached the exact solution closely. Table 2 shows that the present solution is always within 1% of that of Cleland and Wilhelm, even for high values of N_{Da}/G_1, where the solution of Trombetta and Happel is as much as 12% high. This suggests that the present analysis is applicable over a much broader range of reaction rates and diffusivities than that of Trombetta and Happel.

Figures 9 and 10 present the point and average Nusselt numbers for several of the conditions analyzed by Trombetta and Happel.

Again, no effort was made to duplicate all the work reported by Trombetta and Happel. In addition to that discussed here, they investigated variations in the input parameters, their applicability to the pyrolysis of hydrocarbons, and the effects of annular reactor geometry.

Evaluation of Unique Capabilities

Several capabilities of the present model are unique. It was determined that the dependence of diffusivity on temperature is negligible over the range of conditions investigated. The ability to specify adiabatic wall conditions, however, leads to very different results than the isothermal wall condition.

The ability to accommodate significant changes in the total molar concentration reflects an extensive improvement over the capabilities of the Rothenberg and Smith model.

Diffusivity Temperature Dependence. The maximum temperature calculated during the present work was less than $1.4T_0$ for an adiabatic exothermic reaction. This would mean an increase by less than a factor of 1.2 for the diffusivity and G_1. Several problems were analyzed with $G_1 = 2$, and no appreciable difference was found when compared with similar problems with $G_1 = 1$. The excellent agreement of the present analysis with that of Rothenberg and Smith shown in Figures 3 and 4 also shows that over the range of conditions studied, the Chapman-Enskog temperature dependence of diffusivity can be safely neglected.

Change in Total Number of Molecules with Inert Diluents. Rothenberg and Smith's analysis applied only for no appreciable change in the total number of molecules ($b = 1$ or $y_o << 1$). Trombetta and Happel's analysis applied for a change in the total number of molecules, but they did not discuss possible effects of inert diluents. Figure 11 shows the effects of diluents and mole change on the axial temperature profile. The broken curves are calculated for $b = 1$ and apply for any value of y_0. The solid curves are calculated for $b = 2$ for values of $y_0 = 1.0$ and $y_0 = 0.1$. For the two values of G_4 selected, the profiles for $b = 2$, $y_0 = 0.1$ may be approximated by the curves for $b = 1$, $y_0 = 1$. For the conditions of $b = 2$, $y_0 = 1.0$, however, the temperature profiles are significantly different.

Figures 12 and 13 present the axial temperature profiles for the condition $b = 2$, $y_0 = 1.0$ for several of the reactions considered by Rothenberg and Smith. Figures 14 and 15 show the behavior of the Nusselt numbers under these conditions; these figures are very similar to figures

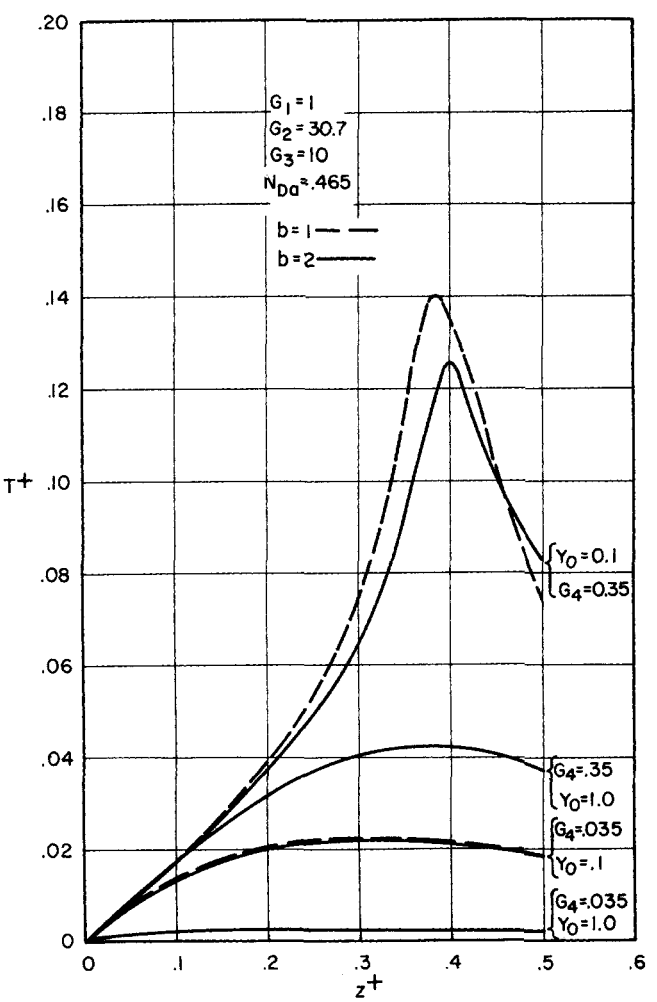

Fig. 11. Comparison of exothermic reactions with concentrated and diluted feed axial temperature profiles.

TABLE 2. COMPARISON OF CORRECTION FACTORS FOR ZERO HEAT OF REACTION

	$N_{Da}/G_1 = 100$				$N_{Da}/G_1 = 10$			
	Present		Cleland Wilhelm	Trombetta Happel	Present		Cleland Wilhelm	Trombetta Happel
y_b^+	$b = 1$	$b = 2$	$b = 1$	$b = 1$	$b = 1$	$b = 2$	$b = 1$	$b = 1$
0.8	1.07	1.09	1.08	1.21	1.03	1.06	1.04	1.06
0.6	1.13	1.16	1.14	1.23	1.07	1.10	1.08	1.08
0.4	1.20	1.20	1.21	1.25	1.10	1.12	1.10	1.10
0.2	1.27	1.25	1.28	1.29	1.13	1.13	1.13	1.13

presented by Rothenberg and Smith for $b = 1$.

Figure 16 shows the correction factors calculated for the same conditions; these too show a similarity to those in Figure 5 calculated for $b = 1$.

The effects of dilution and total mole change are thus significant and should be considered in any application of this analysis.

Adiabatic Boundary Condition. The use of an adiabatic reactor in industrial applications is rare because of possible poor product selectivity, pyrolytic decomposition in exothermic reactions, and self-quenching of endothermic reactions. Analysis of such a problem, however, demonstrates the ability of the present technique to handle a variety of boundary conditions which may be sometime expanded to include more realistic representations.

Figures 17 and 18 present radial temperature and composition profiles for an adiabatic exothermic reaction. Any approximation of the profiles near the completion of the reaction appears quite difficult; a least-squares fit to Equation (44) is shown.

Figure 19 shows the axial temperature and composition profiles for the same reaction, including bulk and wall temperatures.

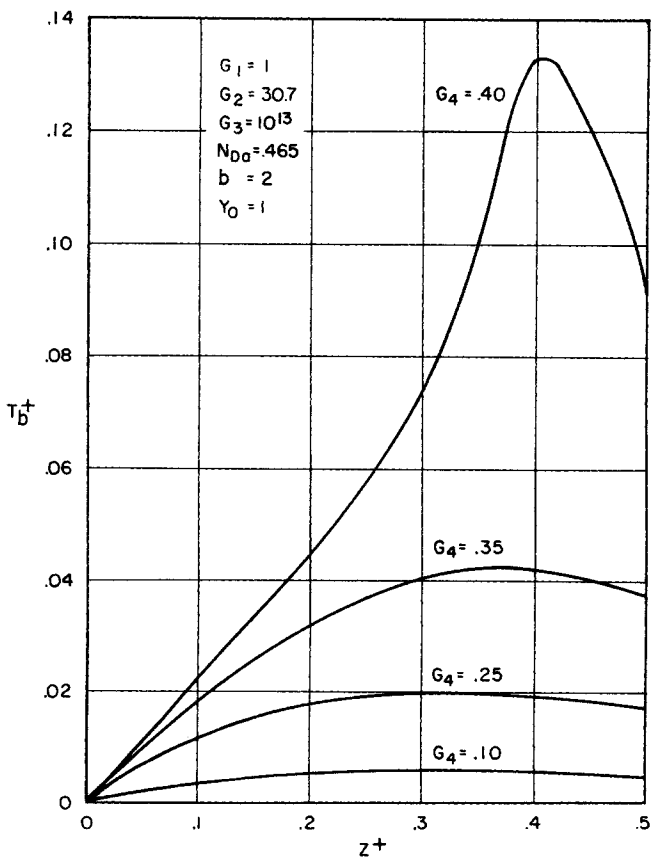

Fig. 12. Axial temperature profiles for exothermic reactions.

It seems quite feasible to combine a heat transfer relation for the wall and surroundings with the present analysis to obtain a realistic thermal boundary condition. Alternatively, continuation type of problems could be run with alternate isothermal and adiabatic boundary conditions for short sections of the reactor.

SUMMARY AND CONCLUSIONS

Summary of New Analyses Performed

1. Correction factor curves have been generated for conditions assumed by Rothenberg and Smith.
2. A complete analysis for conditions assumed by Rothenberg and Smith has been performed with $b = 2$.
3. Radial and axial temperature and concentration profiles have been generated for conditions assumed by Trombetta and Happel. Their power-series approximations did not provide a good least-squares fit to some radial profiles.

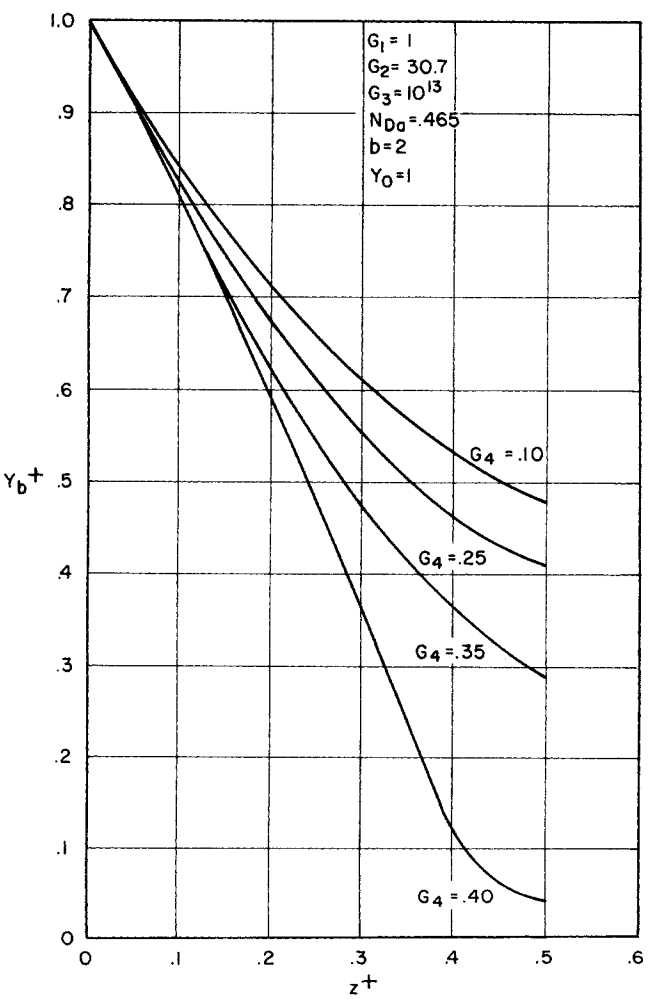

Fig. 13. Axial reactant concentration profiles for exothermic reactions.

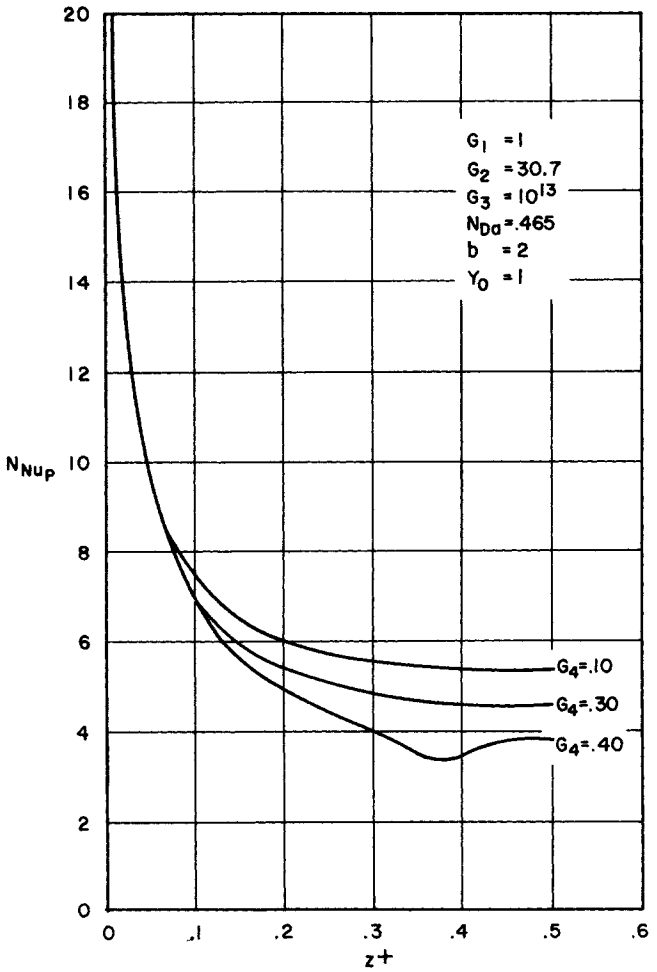

Fig. 14. Point Nusselt numbers for exothermic reactions.

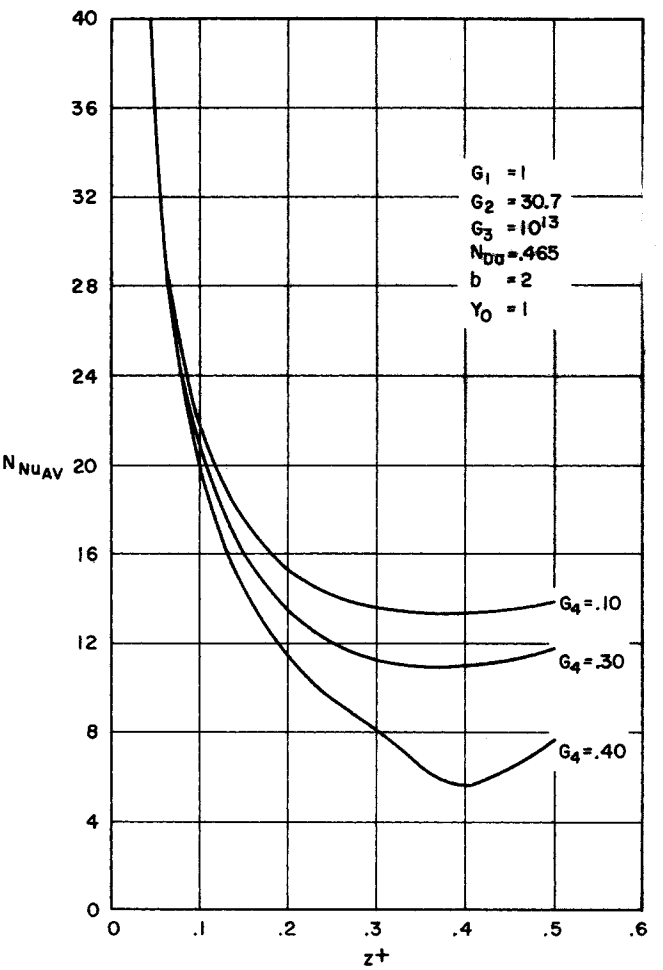

Fig. 15. Average Nusselt numbers for exothermic reactions.

4. Axial Nusselt number profiles have been generated for conditions assumed by Trombetta and Happel.

5. A tubular reactor with adiabatic walls was analyzed.

6. The combined effects of total mole change and feed dilution were studied.

Conclusions

1. The present analysis shows excellent agreement with the calculations reported by Rothenberg and Smith.

2. The present analysis can accommodate changes in the total number of moles which were not considered by Rothenberg and Smith for the case of concentrated feed.

3. The basic analytical difference between the present approach (also Rothenberg and Smith's) and that of Trombetta and Happel is the numerical solution technique: finite difference vs. polynomial approximation.

4. The method of Rothenberg and Smith gives results very close to those of Trombetta and Happel for no significant change in total number of moles.

5. The present extension of the method of Rothenberg and Smith shows good agreement with all conditions reported for a tubular reactor by Trombetta and Happel, including reactions with significant change in the total number of moles.

6. The present analysis showed excellent agreement (better than did the solution of Trombetta and Happel) with the calculations of Cleland and Wilhelm for zero heat of reaction.

The conditions assumed for the present analysis as well as those published earlier are rather extreme idealizations of the conditions to be found in commercial reactors. Use of the correction factors developed here, as well as by Trombetta and Happel, can be used only as guidelines for reactor design. The assertion of stoichiometric diffusion may have to be replaced by ternary diffusion equations for rigorous analysis of feeds which are neither very dilute nor very concentrated. If a precise design technique is required, the present analysis must be expanded to handle real operating conditions of varying wall temperature, inlet mixing effects, reversible and simultaneous reactions, as well as many others.

ACKNOWLEDGMENT

The authors wish to express sincere appreciation to the

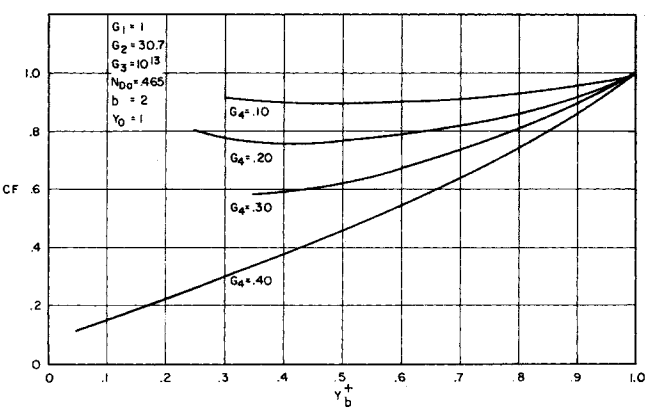

Fig. 16. Correction factors for exothermic reactions.

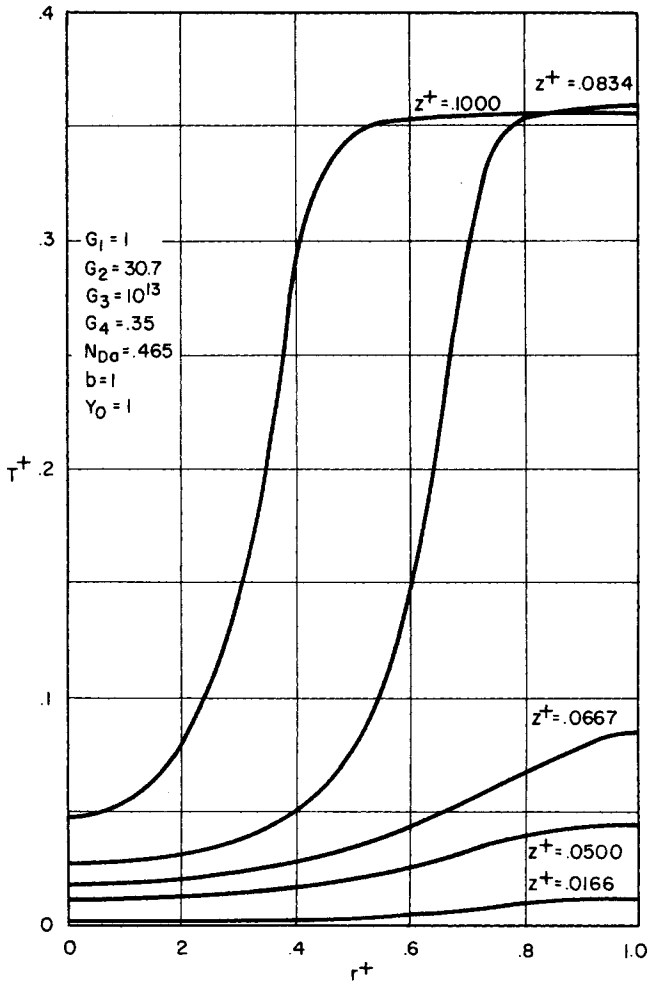

Fig. 17. Radial temperature profiles for an adiabatic exothermic reaction.

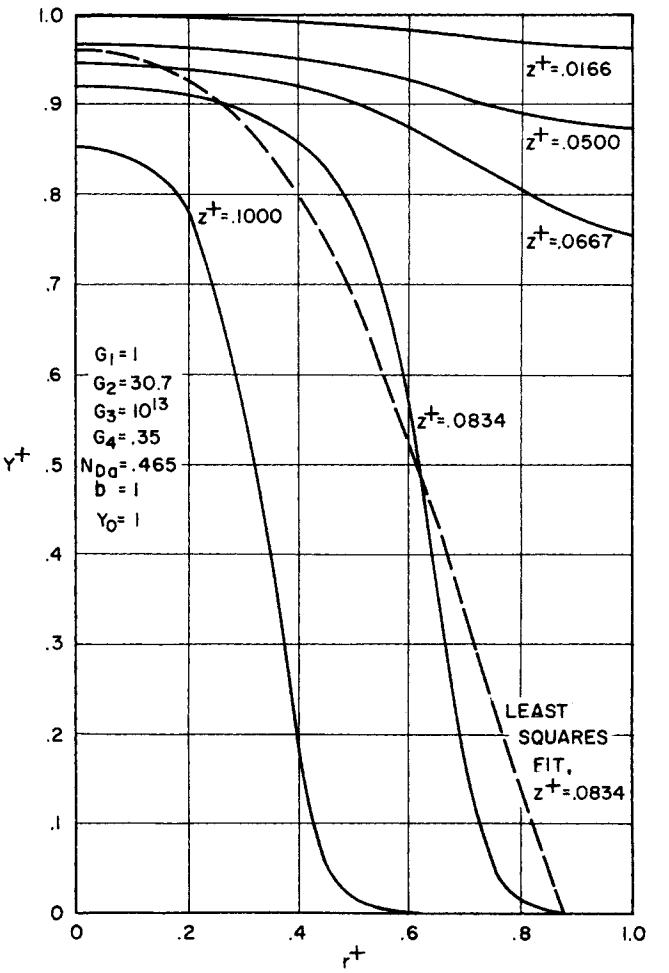

Fig. 18. Radial reactant concentration profiles for an adiabatic exothermic reaction.

National Science Foundation for grant number G-11309, to the University of Pittsburgh Computing Center which made this analysis possible, and to the United States Atomic Energy Commission and Westinghouse Electric Corporation for financial support under the Bettis Doctoral Program.

NOTATION

A = reactant species
B = product species
b = stoichiometric coefficient
$\tilde{c}_p$ = molar heat capacity at constant pressure, cal./g. mole °K.
CF = correction factor
c = molar concentration, (g. moles)/cc.
c_p = specific heat capacity at constant pressure, cal./(g.)(°K.)
D = diffusivity, sq.cm./sec.
E = activation energy, cal./(g. mole)
F = frequency factor, sec.$^{-1}$
G = average velocity, w/ρ (cm.)/(sec.)
G_1 = Lewis number, $c_p M_0 c D^0_{AB}/k$
G_2 = dimensionless activation energy group, $E/R_g T_0$
G_3 = dimensionless frequency factor group, $R_o^2 M_0 c_p P_T F/k$
G_4 = dimensionless heat of reaction group, $-\Delta H\, y_0/M_0\, c_p\, T_0$
H = partial molar enthalpy, cal./(g. mole)
J = diffusive molar flux, (g. moles)/(sq.cm.)(sec.)
K = reaction rate constant, sec.$^{-1}$
k = thermal conductivity, cal./(°K.) (cm.^{1}) (sec.)
M = molecular weight, (g.)/(g. mole)
N = total molar flux, (g. moles)/(sec.) (sq.cm.)
N_{Da} = Damkohler number, $G_3 \exp(-G_2)$
N_{Pr} = Prandtl number, $c_p\mu/k$
N_{Re} = Reynolds number, $2R_o\, w/\mu$
N_{Sc} = Schmidt number, $\mu/\rho D$
N_{Nu} = Nusselt number, $2R_o\, q/k\Delta T$
p = pressure, dyne/sq.cm.
q = heat flux, cal./(sq.cm.)(sec.)
R = reaction generation rate, (g. mole)/(cc.) (sec.)
R_o = reactor radius, cm.
R_g = ideal gas constant, cal./(g. mole) (°K.)
r = radial position vector, cm.
T = absolute temperature, °K.
t = time, sec.
v = mass average velocity, cm./sec.
v^* = molar average velocity, cm./sec.
w = total mass flux, g./(sq.cm.)(sec.)
y = reactant mole fraction
Z_1-Z_{12} = coefficients in power series
z = axial position vector, cm.
μ = viscosity, centipoise
ρ = density, (g.)(cm.$^{-3}$)
ξ = extent of reaction

Subscripts

A = reacting substance
a = average value
B = product substance
b = bulk value
I = inert

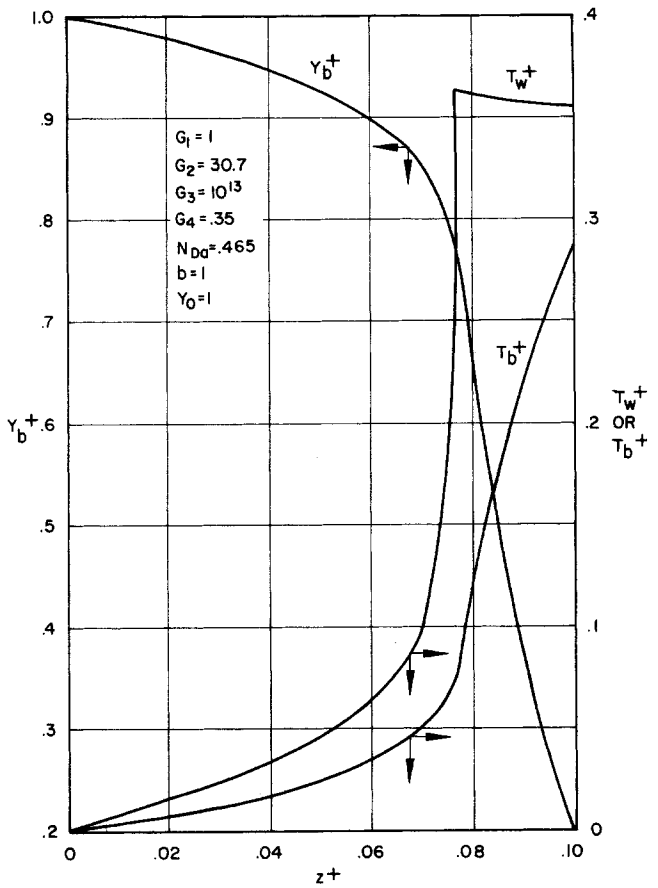

Fig. 19. Axial temperature and concentration profiles for an adiabatic exothermic reaction.

i = substance i
o = initial condition
p = point value
R_o = evaluated at wall
r = radial component
z = axial component

Superscripts

$+$ = dimensionless variable
$''$ = plug flow value
0 = entrance value

Operators

d = ordinary derivative
∂ = partial derivative
Δ = delta, change or increment
Σ_i = summation operator

LITERATURE CITED

1. Hougen, O. A., and K. M. Watson, "Chemical Process Principles," Vol. 3, Wiley, New York (1950).
2. Sandler, Samuel, and Yu Ho Chung. *Ind. Eng. Chem.*, **53**, 391-394 (1961).
3. Steacie, E. W. R., and I. E. Puddington, *Can. J. Res.*, **16B**, 176-193 (1938).
4. Cleland, F. A., and R. H. Wilhelm, *AIChE J.*, **2**, 489-497 (1956).
5. Trombetta, M. L., and John Happel, *ibid.*, **11**, 1041-1050 (1965).
6. Rothenberg, R. I., Ph.D. dissertation, Univ. Calif., Davis (1964).
7. Andersen, T. S., M.S. thesis, Univ. Pittsburgh, Pa. (1967).
8. Bird, R. B., W. E. Stewart, and E. W. Lightfoot, "Transport Phenomenon," Wiley, New York (1960).
9. Lapidus, Leon, "Digital Computation for Chemical Engineers" McGraw-Hill, New York (1962).

Manuscript received May 8, 1968; revision received December 16, 1968; paper accepted December 18, 1968.

Heterogeneous Reactions in the Photochlorination of Propane

BRUNO BOVAL and J. M. SMITH

University of Californ' Davis, California

An experimental study of the photochlorination of propane was undertaken to assess the significance of heterogeneous termination steps (wall reactions). Data were obtained in 2- and 10-mm. I.D. tubular flow reactors with varying oxygen concentrations. The results indicated that homogeneous terminations were dominant in the large reactor, and heterogeneous ones were dominant in the small unit. A kinetic scheme which explained the data was proposed. It included two parallel termination steps: a second-order homogeneous reaction between $C_3H_7\cdot$ and oxygen and a first-order heterogeneous reaction between $C_3H_7\cdot$ and the reactor wall.

Even though the data were taken in the laminar flow regime, the rate of reaction was a function of Reynolds number for the 10-mm. reactor. Kinetic factors may explain these results, but the reasons are not clear. More research in this area is needed.

Data taken in the 10-mm. reactor packed with quartz cylinders gave results similar to those for the 2-mm. reactor. This provided confirming evidence for the proposed scheme of parallel, heterogeneous and homogeneous termination steps.

There is compelling evidence (*12* to *14*) that photochlorinations occur by free radical, chain reactions in which termination steps may be heterogeneous as well as homogeneous. The significance of heterogeneous reactions is particularly important in scaling-up tubular-flow photoreactors because of the variation in surface-to-volume ratio